

Pion-nucleus scattering at high energies

Victor Franco

Physics Department, Brooklyn College of the City University of New York, Brooklyn, New York 11210

Hans Gerd Schlaile

Institut für Theoretische Kernphysik, University of Karlsruhe, D-7500 Karlsruhe 1, Federal Republic of Germany

(Received 10 November 1989)

Elastic scattering of positive and negative pions by nuclei has been analyzed by means of Glauber theory. The full multiple scattering series is calculated, including effects of the Coulomb interaction and inner Coulomb corrections. Double and quadruple charge exchange contributions to the elastic scattering differential cross sections are also included. Applications are made to scattering by ^{12}C and ^{40}Ca . Comparisons are made with measurements at 674 MeV.

I. INTRODUCTION

In past years much attention has been given to the interaction of pions with nuclei.¹ Most measurements have been made at pion kinetic energies below ~ 300 MeV, where the influence of the strong $\Delta(1232)$ resonance in the pion-nucleon interaction is dominant. At significantly higher energies this resonance no longer dominates and more partial waves contribute significantly to pion-nucleon scattering.

Recently precise measurements of pion-nucleus elastic scattering at a kinetic energy well above 300 MeV have been reported.² Such measurements allow the testing of theories which are expected to be more suitable at high energies. One such theory is the Glauber approximation. In this work we use the Glauber approximation to describe pion-nucleus scattering. Effects of the Coulomb interaction are included, as are inner Coulomb corrections and elastic double and quadruple charge exchange corrections.

In Sec. II we describe the theory used in our analysis. In Sec. III we consider two representative nuclear densities. In Sec. IV we compare our calculations with measurements.

II. THEORY

In Glauber theory, the amplitude for hadron-nucleus elastic scattering may be expressed in the simple form³

$$F(q) = ik \int_0^\infty J_0(qb) (1 - e^{i\chi(b)}) b db, \quad (2.1)$$

where k is the incident momentum, q is the momentum transfer, and $\chi(b)$ is an optical phase shift function of the impact parameter b . (We use units in which $\hbar = c = 1$.)

This optical phase shift function may, in turn, be expressed in terms of a phase shift function, χ_c , involving the Coulomb interaction and a phase shift function, χ_s , involving the strong interaction,⁴

$$\chi(b) = \chi_c(b) + \chi_s(b). \quad (2.2)$$

In order to avoid difficulties in the numerical integration subsequently used to evaluate Eq. (2.1) which arise from the long range Coulomb interaction, it is convenient to write the scattering amplitude in terms of a pure Coulomb amplitude, F_c , and an amplitude, F_{cs} , which depends on both the Coulomb and strong interactions,

$$F(q) = F_c(q) + F_{cs}(q), \quad (2.3)$$

where

$$F_c(q) = ik \int_0^\infty J_0(qb) b (1 - e^{i\chi_c(b)}) db, \quad (2.4)$$

and

$$F_{cs}(q) = ik \int_0^\infty J_0(qb) b e^{i\chi_c(b)} (1 - e^{i\chi_s(b)}) db. \quad (2.5)$$

The strong interaction optical phase shift function is given *approximately* by $\chi_s^{(1)}$, with

$$i\chi_s^{(1)}(b) = -\frac{1}{2\pi ik} \int d^2q e^{-iq \cdot b} S(q) \times [Zf_p(q) + (A - Z)f_n(q)], \quad (2.6)$$

where A is the mass number of the target nucleus, Z is its atomic number, f_p and f_n are the amplitudes for elastic scattering of the incident pion by protons and neutrons, respectively, and $S(q)$ is the nuclear ground state form factor. The Coulomb phase shift function may be expressed, for example, in the form

$$i\chi_c(b) = 2i\eta \left\{ \ln(b/2d) + 4\pi \int_b^\infty dr' \rho(r') r'^2 \left[\ln \left[\frac{1 + [1 - (b/r')^2]^{1/2}}{b/r'} \right] - [1 - (b/r')^2]^{1/2} \right] \right\}, \quad (2.7)$$

with

$$\eta = ZZ_\pi \alpha E / k ,$$

where d is an arbitrary constant, $\alpha = e^2 \simeq 1/137.036$ is the fine structure constant, E is the asymptotic energy of the pion, $Z_\pi e$ is its charge, and $\rho(r)$ is the nuclear ground state charge density normalized to unity.

A more accurate representation of the pion-nucleus scattering amplitude may be obtained by summing the Glauber multiple scattering series. The strong interaction optical phase shift function is then given by⁵

$$e^{i\chi_s(b)} = (1 - \Gamma_p)^Z (1 - \Gamma_n)^{A-Z} + \epsilon(b) , \quad (2.8)$$

with

$$\Gamma_j = \frac{1}{2\pi i k_{\pi N}} \int e^{-iq \cdot b} S(q) f_j(q) d^2 q , \quad j = n, p , \quad (2.9)$$

and where $\epsilon(b)$ is a correction due to double and quadruple charge exchange, discussed below. For very heavy nuclei and very high energies the two results Eqs. (2.6) and (2.8) will not yield significant differences in the cross

$$\epsilon(b) = -\frac{1}{4} Z (\Gamma_p - \Gamma_n)^2 \left\{ 1 - (Z-1) \left[\Gamma_p + \Gamma_n - \frac{1}{2} (Z-2) (\Gamma_p + \Gamma_n)^2 - \Gamma_p \Gamma_n + \frac{1}{24} (\Gamma_p - \Gamma_n)^2 \right] \right\} . \quad (2.10)$$

Multiple charge exchange contributions involving quintuple and higher order multiple collisions are negligible and are not included in the present analysis.

For spinless nuclear targets the amplitudes in Eq. (2.9) may, to a fair approximation, be taken to be the non-spin-flip πN amplitudes, and at high energies may be parametrized by

$$f_j(q) = (i k_{\pi N} \sigma_j / 4\pi) (1 - i\alpha_j) e^{-(1/2)a_j q^2} , \quad j = n, p , \quad (2.11)$$

where σ_j is the corresponding πN total cross section, α_j is the ratio of real to imaginary part of the corresponding

$$\Gamma_j = [\sigma_j (1 - i\alpha_j) / 8\pi^2] \int d^2 q d^2 s e^{iq \cdot (s-b)} \rho_A(s) e^{-(1/2)a_j q^2} , \quad j = n, p , \quad (2.14)$$

$$= [\sigma_j (1 - i\alpha_j) / 2a_j] e^{-b^2/2a_j} \int_0^\infty \rho_A(s) e^{-s^2/2a_j} I_0(bs/a_j) s ds . \quad (2.15)$$

For low energy pion-nucleus scattering the inner Coulomb effects⁸ are quite important. As the incident energy increases, these effects decrease in importance. In Glauber theory the effects are twofold.⁸ First, the pion-nucleon parameters must be evaluated at the local energy

$$E_R = E [1 - (k/E)^2 \delta] , \quad (2.16)$$

with

$$\delta = ZZ_\pi \alpha E / k^2 R , \quad (2.17)$$

in which $R = \langle r^2 \rangle^{1/2}$ is the rms radius of the target nu-

sections at very small momentum transfers. But for lighter nuclei, energies that are not very high, or momentum transfers away from the forward direction, the effects can be significant.⁶

The present analysis includes multiple charge exchange contributions to the elastic scattering. For example, multiple collisions such as $\pi^- p \rightarrow \pi^0 n$ followed by $\pi^0 n \rightarrow \pi^- p$, with the nucleus remaining in its ground state after the collision, are included. Multiple charge exchange collisions are included through fourth-order multiple scattering, i.e., through quadruple scattering. Consequently the possibility of quadruple charge exchange (i.e., of quadruple collisions involving four successive charge exchange scatterings) is also included. Since our applications will be to ¹²C and ⁴⁰Ca, in our calculation of $\epsilon(b)$ we assume, for simplicity, that the neutrons and protons are bound in pairs of isotopic spin zero and generalize the techniques used earlier to investigate charge exchange effects in hadron-deuteron collisions.⁷ The contribution of these multiple charge exchange collisions to $e^{i\chi_s(b)}$ is found to be

πN forward scattering amplitude, and a_j is the "slope parameter" of the corresponding πN scattering amplitude. In general, this slope parameter will be complex,

$$a_j = B_j + iG_j . \quad (2.12)$$

If we define

$$\rho_A(s) \equiv \int_{-\infty}^{\infty} \rho_A(s, z) dz , \quad (2.13)$$

where $\rho_A(s, z)$ is the nuclear ground state density of the target, we may express the phase shift function χ_s by Eqs. (2.8) and (2.10) with

cleus. Second, the impact parameter and momentum in the phase shift function are scaled according to

$$b_R = (1 + \delta) b \quad (2.18)$$

and

$$k_R = k / (1 + \delta) . \quad (2.19)$$

We will denote by $\tilde{\chi}$ such Coulomb-corrected phase shift functions. Thus the Coulomb phase shift function becomes

$$i\tilde{\chi}_c(b) = 2i\eta_R \left\{ \ln \left[\frac{b(1+\delta)}{2d} \right] + 4\pi(1+\delta)^3 \int_b^\infty dr \rho[r(1+\delta)] r^2 \left[\ln \left[\frac{1 + [1 - (b/r)^2]^{1/2}}{b/r} \right] - [1 - (b/r)^2]^{1/2} \right] \right\} , \quad (2.20)$$

where

$$\eta_R = ZZ_\pi \alpha E_R / k_R . \quad (2.21)$$

The strong interaction phase shift function becomes

$$e^{i\tilde{\chi}_s(b)} = (1 - \tilde{\Gamma}_p)^Z (1 - \tilde{\Gamma}_n)^{A-Z} \\ - \frac{1}{4} Z (\tilde{\Gamma}_p - \tilde{\Gamma}_n)^2 \left\{ 1 - (Z-1) [\tilde{\Gamma}_p + \tilde{\Gamma}_n - \frac{1}{2}(Z-2)(\tilde{\Gamma}_p + \tilde{\Gamma}_n)^2 - \tilde{\Gamma}_p \tilde{\Gamma}_n + \frac{1}{24}(\tilde{\Gamma}_p - \tilde{\Gamma}_n)^2] \right\} , \quad (2.22)$$

with

$$\tilde{\Gamma}_j = \left[\frac{1}{2} \sigma_j(E_R) / a_j(E_R) \right] [1 - i\alpha_j(E_R)] \\ \times e^{-(1+\delta)^2 b^2 / 2a_j(E_R)} \int_0^\infty \rho_A(s) e^{-s^2 / 2a_j(E_R)} I_0[(1+\delta)bs / a_j(E_R)] s ds, \quad j = n, p . \quad (2.23)$$

These phase shift functions may be evaluated for any given nuclear density distribution.

To summarize, the scattering amplitude for pion-nucleus elastic scattering is given by Eqs. (2.3)–(2.5). In the absence of inner Coulomb corrections, χ_c and χ_s are given by Eqs. (2.7)–(2.10). If the πN amplitudes are Gaussian, the Γ 's are given by Eq. (2.15). If inner Coulomb corrections are made, the Coulomb and strong interaction phase shift functions are given by Eqs. (2.20), (2.22), and (2.23).

III. PHASE SHIFT FUNCTIONS FOR SPECIFIC NUCLEAR DENSITIES

In the present work we shall consider two forms of nuclear density, the three-parameter Fermi density, $\rho_{3pF}(r)$, and the modified harmonic oscillator density, $\rho_{MHO}(r)$.

A. Three-parameter Fermi density

The three-parameter Fermi model is given by

$$\rho_{3pF}(r) = \frac{\rho_0 (1 + wr^2/c^2)}{1 + \exp[(r-c)/a]} . \quad (3.1)$$

The normalization constant, ρ_0 , is calculated to be

$$\rho_0 = \frac{3}{4\pi c^3} \left\{ 1 + \frac{3w}{5} + \left[\frac{\pi a}{c} \right]^2 (1+2w) + \left[\frac{\pi a}{c} \right]^4 \frac{7w}{5} - 6 \left[\frac{a}{c} \right]^3 \sum_{m=1}^{\infty} \frac{(-1)^m}{m^3} \left[1 + \frac{12w}{m^2} \left[\frac{a}{c} \right]^2 \right] e^{-mc/a} \right\}^{-1} . \quad (3.2)$$

The function $\rho_A(s)$ may be obtained from the relation

$$\rho_A(s) = 2\rho_0 \int_0^\infty \frac{1 + w(s^2 + z^2)/c^2}{1 + \exp\{(s^2 + z^2)^{1/2} - c\}/a} dz \quad (3.3)$$

by numerical integration. The phase shift functions χ_s (or $\tilde{\chi}_s$) and χ_c (or $\tilde{\chi}_c$) may be obtained from Eqs. (2.8), (2.10), (2.15), and (2.7) [or from Eqs. (2.22), (2.23), and (2.20)] by numerical integration. The pure Coulomb scattering amplitude may be obtained most conveniently by extracting the point Coulomb amplitude from Eq. (2.4). The result is

$$F_c(q) = -(2\eta_R k / q^2) \\ \times \exp(-2i\{\eta_R \ln[qd/(1+\delta)] + \sigma_0\}) \\ + ik \int_0^\infty b J_0(qb) \exp\{2i\eta_R \ln[b(1+\delta)/2d]\} \\ \times (1 - e^{i\tilde{\chi}_c(b)}) db , \quad (3.4)$$

where

$$\sigma_0 = -\arg\Gamma(1 + i\eta_R) \quad (3.5)$$

and

$$\tilde{\chi}_c(b) = 8\pi\eta_R\rho_0(1+\delta)^3 \int_b^\infty \frac{\left[1 + \frac{wr^2}{c^2}(1+\delta)^2 \right] r^2 \left[\ln \left[\frac{1 + [1 - (b/r)^2]^{1/2}}{b/r} \right] - [1 - (b/r)^2]^{1/2} \right]}{1 + e^{-c/a} e^{r(1+\delta)/a}} dr . \quad (3.6)$$

The integrals are evaluated numerically. The scattering amplitude $F(q)$ may be obtained from Eq. (2.1) by numerical integration.

B. Modified harmonic oscillator density

The modified harmonic oscillator model is given by

$$\rho_{MHO}(r) = \rho_{OM} (1 + \alpha_M r^2 / a_M^2) e^{-r^2/a_M^2} , \quad (3.7)$$

with

$$\rho_{OM} = (\pi a_M^2)^{-3/2} (1 + \frac{3}{2}\alpha_M)^{-1} . \quad (3.8)$$

The function $\rho_A(s)$ is given by

$$\rho_A(s) = 2\rho_{OM} \int_0^\infty [1 + \alpha_M(s^2 + z^2)/a_M^2] \\ \times e^{-s^2/a_M^2} e^{-z^2/a_M^2} dz , \quad (3.9)$$

$$= \left\{ (1 + \frac{1}{2}\alpha_M + \alpha_M s^2 / a_M^2) / [\pi a_M^2 (1 + \frac{3}{2}\alpha_M)] \right\} \\ \times e^{-s^2/a_M^2} . \quad (3.10)$$

The phase shift function $\chi_s(b)$ is obtained from Eqs. (2.8), (2.10), and (2.15), which lead to the simple analytic result

$$\Gamma_j(b) = \left\{ \sigma_j (1 - i\alpha_j) / [2a_j \pi a_M^2 (1 + 3\alpha_M/2)] \right\} e^{-b^2/2a_j} \\ \times \int_0^\infty e^{-s^2[(1/2)a_j^{-1} + a_M^{-2}]} \\ \times (1 + \frac{1}{2}\alpha_M + \alpha_M s^2/a_M^2) I_0(bs/a_j) s ds, \quad (3.11)$$

$$= \frac{\sigma_j (1 - i\alpha_j) e^{-b^2/(2a_j + a_M^2)}}{2\pi(1 + 3\alpha_M/2)(2a_j + a_M^2)} \\ \times \left[1 + \frac{\alpha_M}{2} + \frac{2\alpha_M a_j}{2a_j + a_M^2} + \frac{\alpha_M a_M^2 b^2}{(2a_j + a_M^2)^2} \right], \quad (3.12)$$

with

$$e^{i\chi_s(b)} = (1 - \Gamma_p)^Z (1 - \Gamma_n)^{A-Z} \\ - \frac{1}{4} Z (\Gamma_p - \Gamma_n)^2 \\ \times \left\{ 1 - (Z-1) \left[\Gamma_p + \Gamma_n - \frac{1}{2}(Z-2)(\Gamma_p + \Gamma_n)^2 \right. \right. \\ \left. \left. - \Gamma_p \Gamma_n + \frac{1}{24}(\Gamma_p - \Gamma_n)^2 \right] \right\}. \quad (3.13)$$

The function $\tilde{\chi}_s(b)$ is obtained from $\chi_s(b)$ by evaluating the πN parameters σ_j, α_j, a_j ($j=n,p$) at the energy E_R and replacing b by $(1+\delta)b$.

The Coulomb phase shift for the case of the modified harmonic oscillator density may be obtained from an expression equivalent to Eq. (2.7), namely

$$i\chi_c(b) = 2i\eta \left[\ln(b/2d) + 2\pi \int_b^\infty s \ln(s/b) \rho_A(s) ds \right], \quad (3.14)$$

where $\rho_A(s)$ is given by Eq. (3.10). The integration may be performed analytically to yield

$$i\chi_c(b) = 2i\eta \left\{ \ln(b/2d) - \frac{1}{2} \text{Ei}(-b^2/a_M^2) \right. \\ \left. + [\alpha_M/(2+3\alpha_M)] e^{-b^2/a_M^2} \right\}, \quad (3.15)$$

where $\text{Ei}(-x)$ is the exponential integral. The pure Coulomb scattering amplitude is given by Eqs. (3.4) and (3.5) with $\tilde{\chi}_e$ given by

$$\tilde{\chi}_e(b) = 2\eta_R \left\{ -\frac{1}{2} \text{Ei}[-b^2(1+\delta)^2/a_M^2] \right. \\ \left. + [\alpha_M/(2+3\alpha_M)] e^{-b^2(1+\delta)^2/a_M^2} \right\}. \quad (3.16)$$

The scattering amplitude $F(q)$ for this case is simply given by the one-dimensional integral Eq. (2.1) which can be evaluated numerically.

IV. COMPARISON WITH MEASUREMENTS

In this section we compare our calculations for π^+ and π^- elastic scattering by ^{12}C and ^{40}Ca at 674 MeV with recent measurements.² The πN parameters σ_j, α_j , and a_j ($j=n,p$) are obtained from πN measurements.^{9,10} If inner Coulomb corrections are ignored ($\delta=0$), the parameters would be those measured at the incident pion

kinetic energy (674 MeV) and are given in the first row of Table I. (The $\pi^\pm n$ parameters are obtained from the $\pi^\pm p$ parameters using charge symmetry.) If inner Coulomb corrections are included, the pion kinetic energy T_R [corresponding to the total pion energy E_R of Eq. (2.16)] at which the parameters are obtained will depend upon the particular type of pion and nucleus involved in the collision. These energies and the corresponding values of the πN parameters are shown in the last four rows of Table I. In the calculations of T_R , the rms radii for ^{12}C and ^{40}Ca were taken to be 2.46 fm and 3.48 fm, respectively.¹¹ The cross sections results vary negligibly with moderate variations (± 0.2 fm) in the radii used to determine T_R .

For ^{12}C we have used the modified harmonic oscillator density Eq. (3.7) and for ^{40}Ca we have used the three-parameter Fermi density Eq. (3.1). The parameters used were those obtained in Ref. 2, namely $\alpha_M=2.33$ and $a_M=1.51$ fm for ^{12}C , and $w=-0.065$, $c=3.671$ fm, and $a=0.507$ fm for ^{40}Ca .

The results for $\pi^\pm + ^{12}\text{C}$ elastic scattering are shown in Figs. 1 and 2. The results for $\pi^\pm + ^{40}\text{Ca}$ elastic scattering are shown in Figs. 3 and 4. The dashed curves are obtained ignoring the Coulomb interaction, inner Coulomb corrections, and elastic multiple charge exchange contributions. The solid curves include the Coulomb interaction, inner Coulomb corrections, and multiple charge exchange corrections. The calculations presented contain

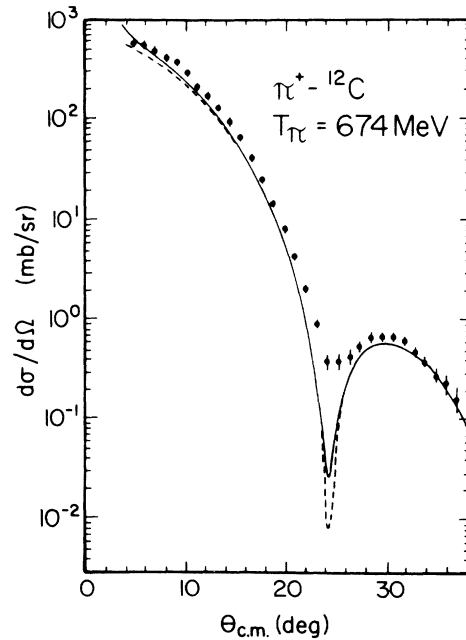


FIG. 1. Differential cross section for $\pi^+ + ^{12}\text{C}$ elastic scattering at 674 MeV incident pion kinetic energy. The data are from Marlow *et al.* (Ref. 2). The dashed curve ignores the Coulomb interaction, inner Coulomb corrections, and multiple charge exchange effects. The solid curve includes the Coulomb interaction, inner Coulomb corrections, and multiple charge exchange corrections.

TABLE I. Pion-nucleon scattering parameters. Total cross sections (σ) and ratios of real to imaginary parts (α) of the forward scattering amplitude are obtained from Ref. 9. The slope parameters (a) are obtained from Ref. 10.

	σ_{π^+p} (mb)	σ_{π^-p} (mb)	α_{π^+p}	α_{π^-p}	a_{π^+p} (GeV/c) ⁻²	a_{π^-p} (GeV/c) ⁻²
$\delta=0, T=674$ MeV	15.33	37.04	-1.078	0.079	1.60-3.24 <i>i</i>	9.52-8.79 <i>i</i>
T_R ($\pi^+ {}^{12}\text{C}$)=671 MeV	15.23	37.37	-1.110	0.070	1.59-3.15 <i>i</i>	9.45-8.70 <i>i</i>
T_R ($\pi^- {}^{12}\text{C}$)=677 MeV	15.44	36.74	-1.045	0.090	1.62-3.31 <i>i</i>	9.69-8.92 <i>i</i>
T_R ($\pi^+ {}^{40}\text{Ca}$)=666 MeV	15.11	37.88	-1.155	0.060	1.53-2.98 <i>i</i>	9.54-8.61 <i>i</i>
T_R ($\pi^- {}^{40}\text{Ca}$)=682 MeV	15.60	36.38	-0.999	0.106	1.76-3.34 <i>i</i>	9.83-8.99 <i>i</i>

no adjustable parameters. The data are from Ref. 2.

In Figs. 1 and 2 it is seen that for $\pi^\pm + {}^{12}\text{C}$ elastic scattering at 674 MeV the combined effects of the Coulomb interaction, inner Coulomb corrections, and multiple charge exchange corrections are rather small (less than $\sim 10\%$) throughout the angular range considered, except at very small angles ($\theta \leq 8^\circ$ for π^+ scattering and $\theta \leq 4^\circ$ for π^- scattering) and near the minimum ($\theta \approx 24^\circ$ – 26°) where the Coulomb interaction makes a significant contribution. The effects of multiple charge exchange are quite negligible, being less than $\sim 1\%$ except near the minimum ($21^\circ \lesssim \theta \lesssim 27^\circ$) and beyond the secondary maximum ($\theta \gtrsim 36^\circ$). Inner Coulomb effects are generally less than ~ 2 – 3% except near the minima. The overall results are seen to be in good qualitative agreement with the data, which vary over four orders of magnitude, with the minimum and secondary maximum occurring at the observed angles in both cases. However there are some quantitative differences between theory and measurements. The calculated results are systematic-

ally lower than the data for $\pi^- + {}^{12}\text{C}$ scattering, and this discrepancy slightly exceeds the overall experimental normalization uncertainty which is $\pm 15\%$. In addition, the minimum is not observed to be so sharp in both cases. It is not unlikely that inclusion of the πN spin flip amplitude would reduce the depth of this minimum.

For $\pi^\pm + {}^{40}\text{Ca}$ elastic scattering at 674 MeV the Coulomb interaction is quite significant. For $\pi^+ + {}^{40}\text{Ca}$ scattering it increases the cross section by at least 10% throughout most of the angular range shown in Fig. 3 (and by much more at some angles). For $\pi^- + {}^{40}\text{Ca}$ scattering, shown in Fig. 4, it increases the cross section by at least 10% (and by much more at some angles) near the forward direction ($\theta \lesssim 4^\circ$), near the first minimum ($\theta \approx 13^\circ$ – 15°), and at larger angles ($\theta \gtrsim 24^\circ$). The effects of multiple charge exchange in $\pi^\pm + {}^{40}\text{Ca}$ scattering are quite negligible, being less than $\sim 1\%$ except near the first minimum ($\theta \approx 13^\circ$ – 17°) and near the second minimum ($\theta \approx 24^\circ$ – 26°). Inner Coulomb effects are generally less than ~ 2 – 3% except near the minima. The re-

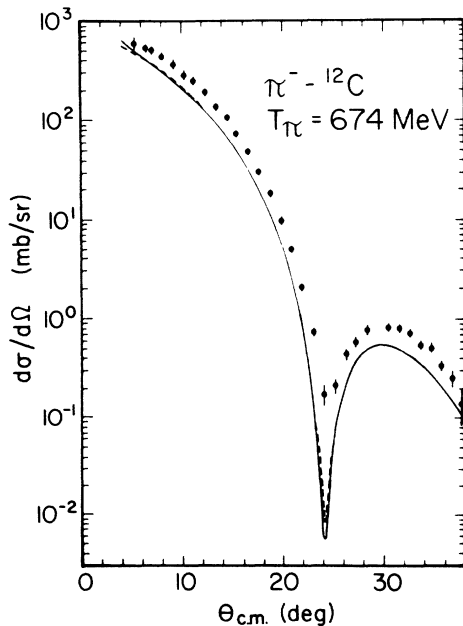


FIG. 2. Same as Fig. 1, but for $\pi^- + {}^{12}\text{C}$.

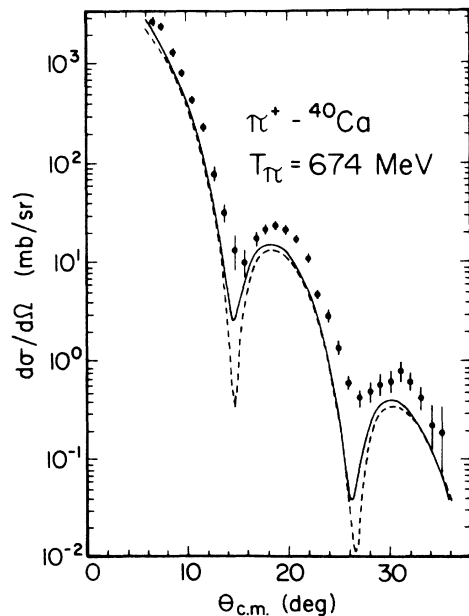


FIG. 3. Same as Fig. 1, but for $\pi^+ + {}^{40}\text{Ca}$.

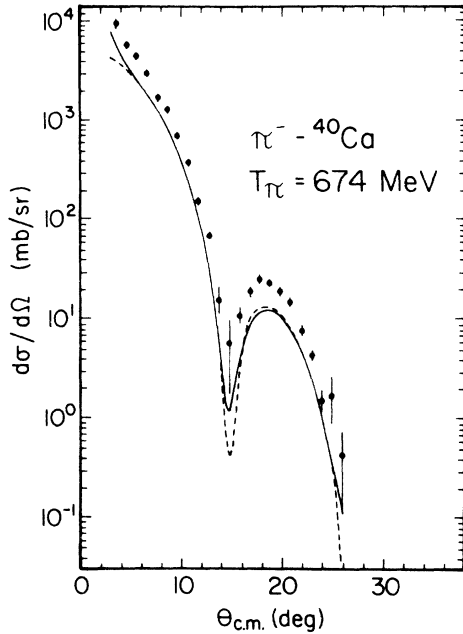


FIG. 4. Same as Fig. 1, but for $\pi^- + {}^{40}\text{Ca}$.

sults are in good qualitative agreement with the data, which vary over almost five orders of magnitude. The maxima and minima occur at the observed angles in both cases. However, the magnitude of the calculated cross sections are systematically too small, typically being $\sim 30\text{--}50\%$ below the observed cross sections. This discrepancy significantly exceeds the $\pm 15\%$ overall ex-

perimental normalization uncertainty. As in the $\pi + {}^{12}\text{C}$ cases, the minima are not observed to be so sharp, and it is not unlikely that inclusion of the πN spin flip amplitude would reduce the depths of the minima.

We might point out, in passing, that there are several other forms for the phase shift function and corresponding profile function Γ that are often used in Glauber theory that are more approximate than Eqs. (2.8) and (2.9). One example, already mentioned, is given by Eq. (2.6). A second may be obtained by ignoring the angle dependence of the basic πN elastic scattering amplitude, thereby allowing the integrations in Eq. (2.14) to be done explicitly. We have performed calculations for $\pi^\pm + {}^{12}\text{C}$ and $\pi^\pm + {}^{40}\text{Ca}$ elastic scattering using each of these more approximate forms in the π -nucleus scattering amplitude. In each case the results obtained are in somewhat better overall agreement with the data. Sometimes an approximation to an approximation gives better numerical results than the original approximation. We believe this to be fortuitous here. It may, however, indicate that these more approximate forms are sufficiently accurate for obtaining reasonable qualitative results. It would be interesting to have similar measurements at higher energies where the theory is expected to be more accurate.

ACKNOWLEDGMENTS

This work was supported in part by the Bundesministerium für Forschung und Technologie and the Professional Staff Congress of the City University of New York (PSC-CUNY) Faculty Research Award Program. One of us (V.F.) wishes to thank Professor H. Pilkuhn and the Institut für Theoretische Kernphysik, where this work was begun, for their kind hospitality.

- ¹W. R. Gibbs and B. F. Gibson, *Annu. Rev. Nucl. Part. Sci.* **37**, 411 (1987); J. M. Eisenberg and D. Koltun, *Theory of Meson Interactions with Nuclei* (Wiley, New York, 1980).
²D. Marlow *et al.*, *Phys. Rev. C* **30**, 1662 (1984).
³R. J. Glauber, in *Lectures in Theoretical Physics*, edited by W. Brittin *et al.* (Interscience, New York, 1959), Vol. I, p. 315.
⁴V. Franco, *Phys. Rev. Lett.* **16**, 944 (1966).
⁵See, for example, V. Franco, *Phys. Rev. Lett.* **24**, 1452 (1970).
⁶See, for example, V. Franco and A. Tekou, *Phys. Rev. C* **37**, 1097 (1988).
⁷R. J. Glauber and V. Franco, *Phys. Rev.* **156**, 1685 (1967).
⁸G. Fäldt and H. Pilkuhn, *Phys. Lett.* **46B**, 337 (1973).
⁹G. Höhler and F. Kaiser, Kernforschungszentrum Karlsruhe Report No. 3027, 1980 (unpublished). These tables were used to obtain the pion-nucleon total cross sections (σ_T) and the

- ratios of real to imaginary parts of the πN forward scattering amplitudes (α_j) by interpolating to the appropriate energies.
¹⁰G. Höhler, F. Kaiser, R. Koch, and E. Pietarinen, *Handbook of Pion-Nucleus Scattering* (Physics Data, No. 12-1, Fachinformationszentrum Energie, Physik, Mathematik, Karlsruhe, 1979). These tables were used to obtain the pion-nucleon slope parameters (a_j) by interpolating the amplitudes to the appropriate energies and fitting the amplitudes for angles smaller than 40° to the form given by Eq. (2.11). These parameters are determined with a theoretical uncertainty of up to approximately 20% since the actual amplitudes are not precisely of the form given by Eq. (2.11).
¹¹C. W. de Jager, H. de Vries, and C. de Vries, *At. Data Nucl. Data Tables* **14**, 479 (1974).